



EFFECT OF WATER VOLUME ON A THERMOELECTRIC COOLER BOX PERFORMANCE

M. Mirmanto*, I.W. Joniarta, I.M.A. Sayoga, N. Nurpatria, Y.A. Padang, I.G.N.K. Yudhyadi

*Mechanical Engineering Department, Engineering Faculty, Mataram University, Mataram, NTB, 83125, Indonesia
Jl. Majapahit no. 62, Mataram, NTB, 83125, Indonesia*

ABSTRACT

Due to rapid demand on the thermoelectric cooler box, an investigation concerning the effect of water volume on a thermoelectric cooler box performance and its *COP* has been conducted. The aim of this study is to know the performance and the *COP* of the cooler box with water volume variations. The conduction heat transfer rate flowing from the ambient to the cooler box space is discussed deeply as this type of heat transfer rate is seldom to be elucidated in the published literature and it can be the dominant of the heat load when there is no water volume inside the cooler box. The cooler box size was 390 mm x 320 mm x 530 mm and the water volume variations employed were ranging from 0 to 4500 ml. The power used was of approximately 51.27 W. The results indicate that increasing the water volume raises the cooler box space temperature and the *COP* but decreases the conduction heat transfer rate. At 0 ml water volume, the conduction heat transfer rate increases and it gets constant, while at higher water volumes the *COP* decreases with the time. The effect of the water volume on the heat transfer rate of the air is negligible but it is significant on the total heat transfer and conduction heat transfer.

Keywords: Cooler box, *COP*, Thermoelectric, Water volume

INTRODUCTION

A cooler box is one of the cooling devices that preserves the freshness of food, vegetable and other goods inside its room and resists the development of microbes/bacteria that cause spoilage. Therefore, many households to save their foods (goods) in order to stand in a longer time commonly use this device. Nevertheless, cooler boxes/ refrigerators those are available till now in the market employ a compression system. This system needs high pressures so that its construction is not compact and it needs high power. Furthermore, this system is usually heavier due to the big construction so that it is difficult for traveling. Hence, it is recommended to find a new concept to have a refrigerator that requires low electrical power, high portability, small space and environmentally friendly. One thing, which may be important to be considered, is a refrigerator run using thermoelectrics, Abdul-Wahab et al. (2009), Jugsujinda et al. (2011), Reddy (2016), Mirmanto et al. (2018a, 2018b).

Thermoelectric studies have been developed whether experimentally or numerically. Nevertheless, this subject is still challenging the researchers due to its lower performances, even less than 1 in term of *COP* (coefficient of performance). For instance, Abdul-Wahab et al. (2009) investigated thermoelectric as the engine to run a refrigerator. They obtained the lowest temperature of around -5°C and the *COP* of 0.161 at the power of 9.5 W. Recently; Rawat et al. (2013) studied the development of the thermoelectric refrigeration. They found the lowest temperature of around 12°C and the *COP* of 0.1 at the power of 19 W. Reddy (2016) examined the hot and the cold sides of the thermoelectric. As the difference temperature increased, the *COP* decreased and finally, the *COP* was less than 1.

It has lower performances but it is important when criteria such as low power, quietness, no leakage problem, the small place needed or

compact, portability, durability and easiness of maintenance become interesting to be investigated further. However, to improve the performance of the thermoelectric is not easy. Studies to improve thermoelectric refrigerator performances have been performed for years, e.g. Ghoshal et al. (2002), Yang et al. (1991) and Lee et al. (2015). Most of them improved the performance of the thermoelectric from its material or its structure. Lu et al. (2014) enhanced their thermoelectric refrigerator by applying materials that had inhomogeneous thermal conductivities. They stated that using this technique could raise the figure of merit, consequently increased the performance of the refrigerator. Some studies exposing improvements of the use of thermoelectric have been published too. Attey (1998) concluded that using low thermal impedance liquid raised the *COP* surprisingly. When using complete solid heat sink the *COP* obtained was 0.4-0.6, while using liquid heat sink the *COP* gained was 0.95-1.85. Yu and Wang (2009) studied enhancing thermoelectric cooling by using internally cascaded thermoelectric couples. They found that this method could increase the *COP* of the cooling system. However, not the enhancement of the refrigerator nor thermoelectric materials that is going to be investigated in this paper but the effect of water volumes on the performance of the refrigerator. By knowing this effect, the way to increase the *COP* of the thermoelectric refrigerator can be detected.

Predicting the performance of the thermoelectric cooler box is quite various. Some studies did not present the actual estimation of the cooling capacity. Meanwhile, this cooling capacity can be different from the theory so that the experimental results may be deteriorated. When the cooling capacity is estimated using the theory, the cooling capacity is considered only on the surface of the cold side of the thermoelectric, while when the actual capacity is used, the cooling capacity is calculated for the entire system. These two different cooling capacities are obviously different.

* Corresponding author Email: m.mirmanto@unram.ac.id

Moreover, one thing that should be noted in calculating the cooling capacity of the thermoelectric cooler box is the conduction heat transfer component. This type of heat transfer affecting greatly the prediction of cooling capacity is seldom reported in the literature. For that, this paper is encouraged to report this type of heat transfer investigation. Atik and Yildiz (2012) calculate the Q_c (cooling load or cooling capacity) based on the theoretical equation, therefore they did not mention the experimental cooling capacity. Manohar et al. (2016) examined the thermoelectric cooler. They already included the conduction heat transfer rate, but without water volume variations. They elucidated that the cooling capacity comprised passive and active cooling capacities. The passive cooling capacity was the conduction heat transfer rate. Jugsujinda et al. (2011) estimated the Q_c for their cooler using theoretical formula, consequently, they did not describe the conduction heat transfer rate. Mirmanto et al. (2018b) considered the conduction heat transfer rate for their thermoelectric cooler box performance calculation; however, they did not vary the water volume.

From the above literature, investigations of the effect of water volume on the performance of the cooler box have not been conducted yet and the conduction heat transfer rate is rarely elucidated in the literature. Furthermore, in the practical works the real cooling capacity, Q_c is different from that of the theory therefore this may deteriorate the concluding remarks of the experimental performance of the cooler box. For that reasons, this study is performed.

2. RESEARCH METHOD

2.1 Experimental Facility and Method

The schematic diagram of the cooler box system is shown in Fig. 1 and the cooler box was made from some material layers, i.e. styrofoam, stainless steel, plastic and hardwood. The LabView program connected to the NI DAQ9714 was used to read and record all sensors or data. Before the DC (direct current) power was turned on, the LabView program should have been run but it should not record anything yet. The cooler box door was open and bottles filled with drinking water varying from 600 ml to 4500 ml were placed in it for each experiment. To have a uniform temperature or thermal balance condition in the cooler box room, the cooler box door was left open for several minutes. After the temperatures of the air and water inside the cooler box room were the same, then the door was closed firmly. By pressing the save button on the LabView, the data was starting to be recorded at every second. While the LabView was saving the data, the DC power was turned on. The LabView continued recording the data until of approximately 21600 seconds.

Three identical thermoelectrics model TC1-12706 were employed in the experiment. The cold side of each thermoelectric was connected to the inner heat sink inside the refrigerator room via copper blocks. Meanwhile, the hot side was joined to the outer heat sink at the outside of the cooler box wall. The specification of the thermoelectric is given in Table 1, while the installation and the construction of the thermoelectric module are presented in Fig. 2.

Table 1 Specification of the TEC1-12706 thermoelectric

| | |
|---------------------------|-----------------|
| Model | TEC1-12706 |
| Voltage (V) | 12 V |
| Vmax (V) | 15.4 V |
| Imax (A) | 6 A |
| Qmax (W) | 92 W |
| ΔT_{max} (°C) | 66 or 75 |
| Internal resistance (Ohm) | 1.98 or +/- 10% |
| Type | Cooling cells |

All temperatures were measured using K-type thermocouples with an uncertainty of $\pm 0.2^\circ\text{C}$ obtained by the calibration performed in a constant temperature oil bath against the RTD thermocouple sensor. Eight thermocouples were placed in the cooler box room, three thermocouples were set on the thermoelectric hot side, other three thermocouples were put on the thermoelectric cold side, ten thermocouples were placed on the inner heat sink and one thermocouple was used to measure the ambient temperature.

The DC power used was measured using a clamp meter model HP-870N with a VDC (volt direct current) accuracy of $\pm 1.5\%$ reading and an ADC (ampere direct current) accuracy of $\pm 3\%$ reading. The VDC measurement range was 6-60 V while the ADC measurement range was 0-600 A. The resolution of the VDC measurement was 1 mV while that of the ADC measurement was 0.1 A. The DC power used was approximate of 51.27 W obtained from 16.5 A of current and 11.49 V of voltage. The thermoelectric modules were arranged in a parallel circuit and the power was gained from three DC adaptors arranged in parallel circuit too.

The cooler box utilized in this current study was made of sandwich walls (multilayer walls). The overall size of the cooler box was 390 mm x 320 mm x 530 mm. Details of the cooler box wall are given in Table 2. Three identical fans installed on the outer heat sink were used to remove the heat away from the outer heatsink. The fan voltage and current were 12 V and 0.15 A respectively.

2.2 Heat Transfer Analysis

As the aim of this study is to know the effect of water volume on the cooler box performance and COP as well as conduction heat transfer rate, then some equations relating to the cooling capacity, conduction heat transfer rate and the COP are adopted. To determine cooling capacity from the air and water in the bottle placed in the cooler box, an equation that was also used by Abdul-Wahab et al. (2009), Ananta et al. (2017), Mirmanto et al. (2018b) can be utilized; however, it should be modified as:

$$Q_{(i)} = m_{(i)} c_{p(i)} \Delta T_{(i)} / (t_i - t_{i-1}) \quad (1)$$

$Q_{(i)}$ is the heat transfer rate from goods in the cooler box room (W) at the time i . $m_{(i)}$ is the mass of the goods cooled at the time i , $c_{p(i)}$ represents the specific heat (J/kgK) and $\Delta T_{(i)}$ is the temperature difference of the goods between the temperature of $T_{(i-1)}$ and the temperature of $T_{(i)}$ at the time i (°C). i runs from 1 to the number of the time segment, n . t is the time of the cooler box running (s).

When the cooler box space starts to be cold down, the conduction heat transfer is prevailing. This heat transfer can be estimated using an equation suggested by Holman (1997) or other heat transfer textbooks and is given by:

$$Q_{k(i)} = -kA \frac{dT_{(i)}}{dx} \quad (2)$$

k is the thermal conductivity (W/m°C). A is the heat transfer area perpendicular to the heat flow (m²). dT is the temperature difference (°C) between the inner and outer wall temperatures, and dx is the thickness of the refrigerator wall (m), see Table 2. However, as the walls of the refrigerator are constructed from several material layers, then Eq. (2) can be rearranged using thermal resistance model as follows:

$$Q_{k(i)} = \frac{(T_{wo(i)} - T_{wi(i)})}{R} \quad (3)$$

$$dT_{(i)} = T_{wo(i)} - T_{wi(i)} \quad (4)$$

$$R = R_1 + R_2 + R_3 \quad (5)$$

$$R_1 = \frac{x_1}{k_1 A} \quad (6)$$

Table 2 Details of the refrigerator walls (dimension of inside room)

| Wall | Length (m) | Width (m) | Height (m) | Materials and thickness, x , (m) | | | | |
|-------------------------------------|------------|-----------|------------|------------------------------------|-----------|---------|-----------|--------------|
| | | | | Stainless steel plate | Styrofoam | Plastic | Hardboard | Polyurethane |
| Left | | 0.235 | 0.447 | 0.0006 | 0.0385 | 0.001 | | |
| Right | | 0.235 | 0.447 | 0.0006 | 0.0385 | 0.001 | | |
| Top | 0.317 | 0.235 | | 0.0006 | 0.0385 | 0.001 | | |
| Bottom | 0.317 | 0.235 | | 0.0006 | 0.0385 | 0.001 | | |
| Back | 0.317 | | 0.447 | 0.0006 | 0.0485 | 0.001 | | |
| Door | 0.317 | | 0.447 | | | 0.001 | 0.02 | 0.0195 |
| Thermal conductivity, k , (W/m K) | | | | 12-45 | 0.03 | 0.03 | 0.15 | 0.03 |

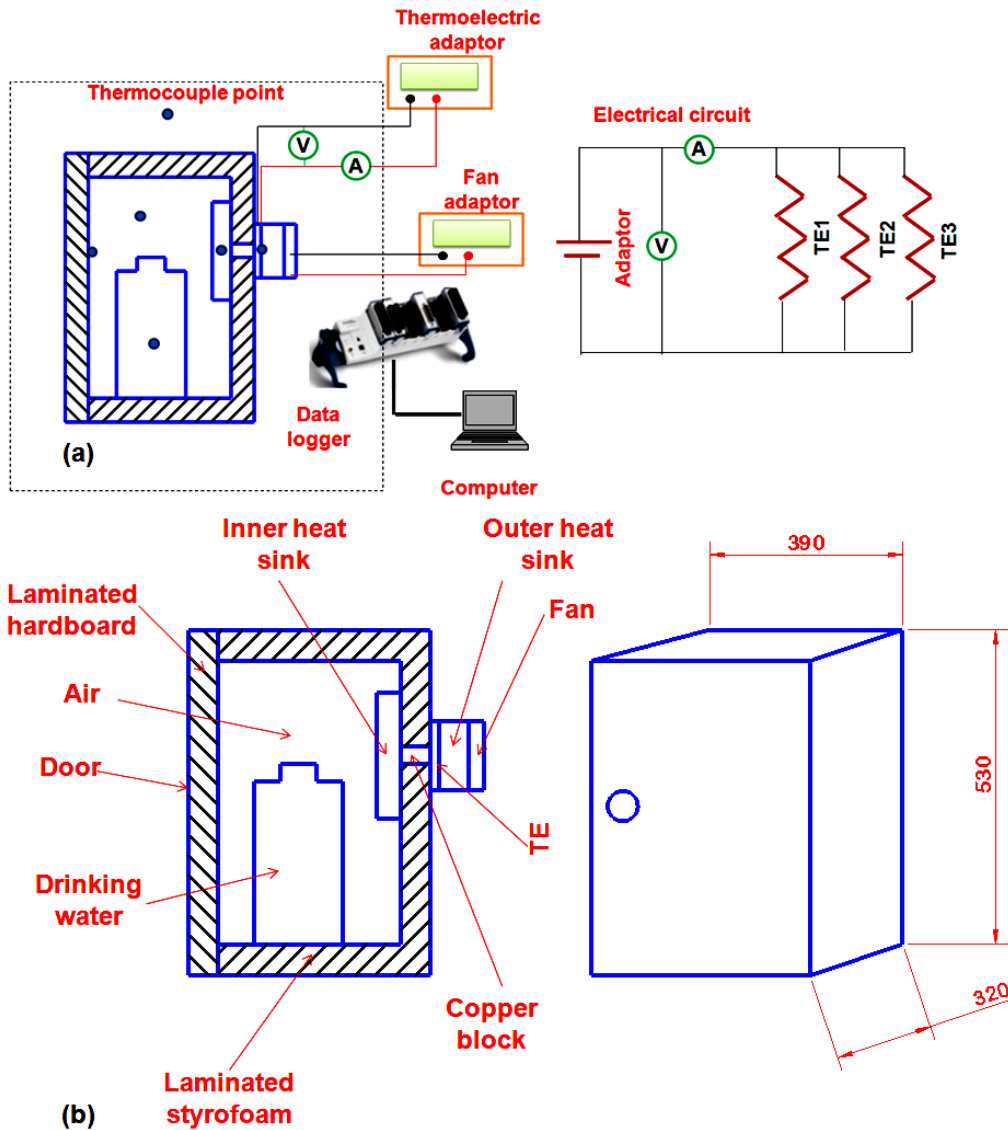


Fig. 1 Research facility: (a) schematic diagram and its electrical circuit, (b) thermoelectric assembly and the refrigerator parts. TE1 to TE3 are the thermoelectric modules, V is the voltmeter and A is the ampere meter.

$$R_2 = \frac{x_2}{k_2 A} \quad (7)$$

$$R_3 = \frac{x_3}{k_3 A} \quad (8)$$

A , x , and k are constant, x is the thickness of the wall (m), T_{wo} is the outer wall surface temperature, while T_{wi} is the inner wall surface temperature. Both temperatures were measured directly in the experiment.

Heat balance in the thermoelectric cooler box system can be predicted as, Cengel and Boles (2006):

$$Q_h = Q_c + P_{in} \quad (9)$$

Q_h is the heat flowing out from the hot side of the thermoelectric to the ambient; Q_c is the heat coming into the cold side of the thermoelectric, It is the same as the total cooling capacity when there is no heat leakage from the ambient to the copper block connectors. p_{in} is the DC power (W) supplied to the thermoelectric. Meanwhile, the input power can be calculated using the equation that was also used in Abdul-Wahab et al. (2009), Mirmanto et al. (2018b) and is expressed as:

$$P_{in} = VI \quad (10)$$

V and I are the voltage (volt) and the current (ampere) supplied to the thermoelectric. One important parameter to evaluate the performance of the thermoelectric cooler box is COP, which can be estimated by applying the equation that was also used by Abdul-Wahab et al. (2009), Mirmanto et al. (2018b):

$$COP = \frac{Q_c}{P_{in}} \quad (11)$$

$$Q_c = Q + Q_{wa} + Q_k \quad (12)$$

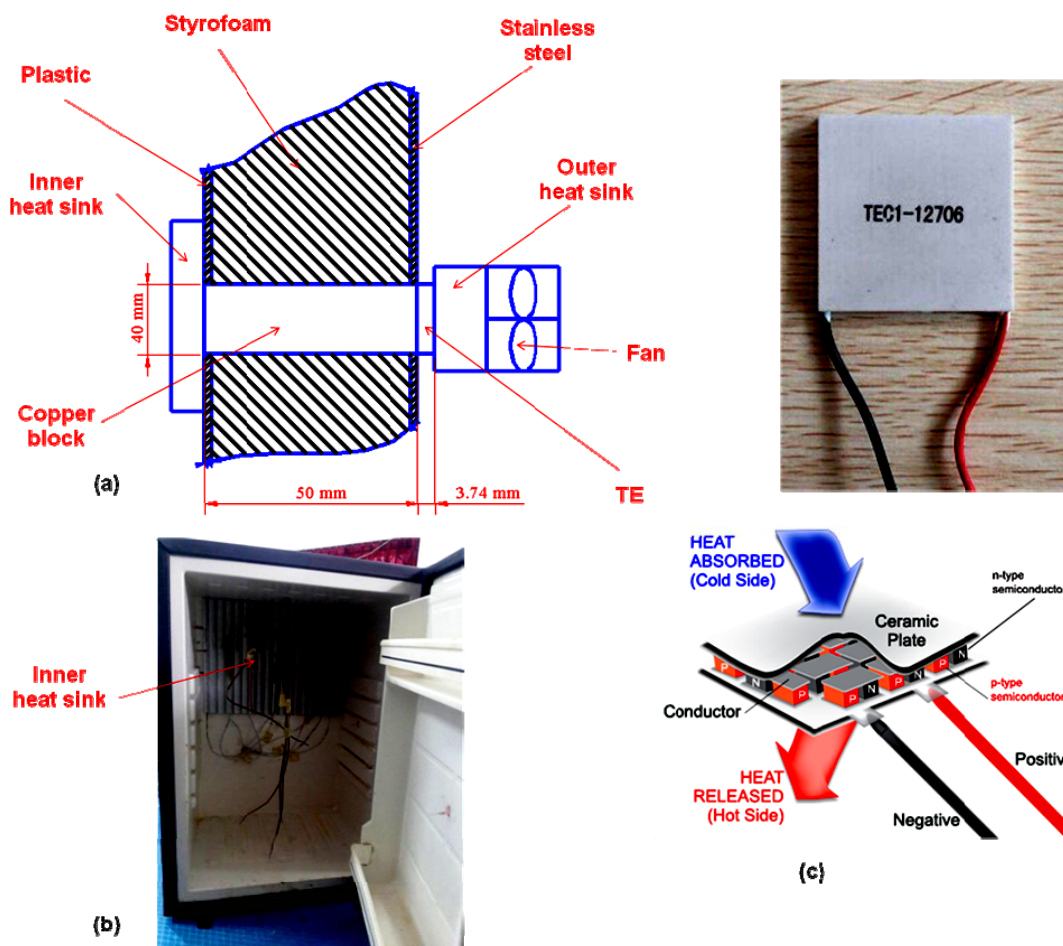


Fig. 2 Thermoelectric: (a) installation, (b) inner heat sink installation, (c) thermoelectric module TEC1-12706

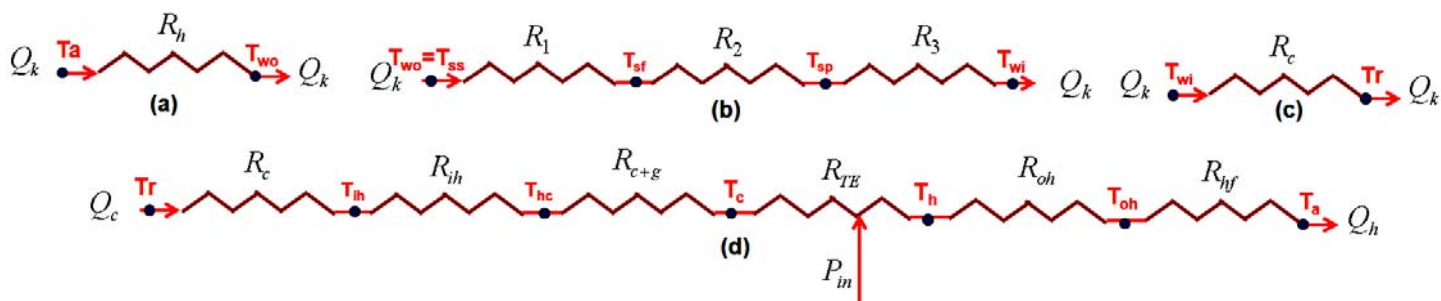


Fig. 3 Thermal resistance circuit; (a) heat flows from the ambient to the outer walls, (b) heat flows from the outer walls to the inner walls, (c) heat flows from inner walls to the air inside the refrigerator, (d) heat flows from the cooler box room to the ambient through the inner heat sink-copper blocks-TE-outer heat sink.

where Q_{wa} is the heat transfer rate from the water inside the cooler box room (W), while Q is the heat transfer rate from the air in the cooler box room. Equation (11) in this study is the experimental *COP*. The conduction heat transfer rate flowing from the ambient through the walls can be illustrated in Fig. 3 in the form of thermal resistance model. The heat transfer rate flows from the ambient to the outer wall surfaces via the free convection heat transfer mode. The thermal resistance for this heat transfer is indicated by R_h . From the outer wall surface, the heat transfer rate flows through the wall layers. The thermal resistances of the wall layers are indicated by R_1 , R_2 , and R_3 . After reaching the inner wall surface, the heat transfer rate flows through the air inside the refrigerator room via the free convection heat transfer mode. The thermal resistance for this heat transfer is noted by R_c . So there are 5 thermal resistances for the heat transfer rate flowing from the ambient to the air inside the refrigerator room. The thermal resistances in Fig. 3(a) and (b) can be arranged as:

$$R_c = \frac{1}{h_c A} \quad (13)$$

$$R_h = \frac{1}{h_h A} \quad (14)$$

R_c is the thermal resistance of the free convection heat transfer inside the cooler box room ($^{\circ}\text{C}/\text{W}$), while R_h is the thermal resistance of the free convection heat transfer outside the cooler box ($^{\circ}\text{C}/\text{W}$). h_c and h_h are the free convection heat transfer coefficients ($\text{W}/\text{m}^2\text{K}$). Therefore, the total thermal resistance, R_t , can be expressed as

$$R_t = R_h + R_1 + R_2 + R_3 + R_c \quad (15)$$

However, in this current study, the T_{wi} and T_{wo} are measured directly so that in calculating the conduction heat transfer, the thermal resistance in Eq. (3) is used instead of Eq. (15). Hence, the thermal resistance circuit in Fig. 3(c) is obviously employed.

3. RESULTS AND DISCUSSION

The experimental results are presented in the form of graphs. Prior to discussing the conduction heat transfer rate, cooling capacity, and the *COP*, the transient temperatures, which are useful for determining the cooling capacity, are plotted to see their trends with the observation time as shown in Fig. 4.

All temperature trends are the same, as the observation time increases the temperature lines decrease, e.g. Tr and Twa , while the ambient temperature, Ta remains constant at all times. This trend was also found by previous researchers, e.g. Jugsujinda et al. (2011), Villasevil et al. (2013), Mirmanto et al. (2018b). These trends were due to the cooler box closed firmly. When the heat is removed from a closed room, then the temperature inside the room decreases till it reaches a thermal equilibrium. This trend was also attained by Manohar and Adeyanju (2014). Their cooling load was water at the initial temperature of around 30°C and the final water temperature was about 5°C after it ran for about 70 minutes. Nevertheless, they only used 325 ml of water. They did not vary the volume of the water. Moreover, the water temperature seems to decrease more fairly than the air temperature. This was due to the plastic bottle that gave restrictions to the heat transferring from the water to the surrounding air inside the cooler box room.

As shown in Figure 5, the room temperature varies at different water volumes. Increasing the water volume increases the room temperature at the same duration of time and power. This phenomenon was due to the increased heat that should be removed from the cooler box room. The heat that can be absorbed by the thermoelectric is persistent depending on the power supplied to it. Therefore, at higher heat, the capability of the thermoelectric at the corresponding power is not enough to remove the heat. Consequently, the temperatures inside the cooler box room increase.

Similarly, the water temperature decreases with the time and the water temperature also increases with the increase in the water volume as shown in Fig. 6. For example at the time of 20000 s, the temperature of 600 ml is almost 15°C , while at 1500 ml, the water temperature is around 16°C , and at 3000 ml and 4500 ml, the water temperatures are approximately 17°C and 19°C . The heat transfer rate from the water increases with the increase in the volume of drinking water. This is due to the increase in the water mass. Increasing the drinking water volume elevates the water mass; therefore it raises the heat transfer rate from the drinking water. This also agrees with Eq. (1) that indicates the effect of the object mass on the heat transfer rate. Figure 7 shows relationships between the observation time and the heat transfer rate from the air at several volumes of drinking water. The cold side thermoelectric has the lowest temperature so that the heat from the cooler box room flows toward the cold side of the thermoelectric. The heat flows through the copper connectors constructed from 10 copper blocks with each size of approximately 4 cm x 4 cm x 0.5 cm, can be seen in Fig. 8. There were 3 copper connectors used in the experiments because there were 3 thermoelectric modules. Then the total copper blocks were of 30 pieces. The air heat transfer rate decreases with the time for all water volume as shown in Fig. 7. At the 0 - 5000 s, it decreases sharply but after 5000 s, it decreases fairly toward zero. The decreased air heat transfer rate is due to the decreased air temperature. When the air temperature reaches a constant value, then the air heat transfer rate reaches zero. The properties of the air used in the calculation are determined from an air property table based on the air bulk temperature. The instantaneous air bulk temperature, $T_{f(i)}$, is estimated using an equation that can be obtained in Holman (1997), however, it should be modified as:

$$T_{f(i)} = (Tr_{(i)} + Tr_{(i-1)}) / 2 \quad (16)$$

Similar to the air heat transfer rate, the water heat transfer rate also decreases with the time as shown in Fig. 9. However, as the volume of drinking water steps up, the water heat transfer rate also elevates. This is due to the increased water mass as explained in the previous paragraph, while the decreased water heat transfer rate is caused by the decreased water temperature along the observation time.

When the air and water heat transfer rates reach the zero value, the conduction heat transfer displays a contradictory phenomenon. It increases with the time. This is because of the decreased room temperature. As the room temperature decreases, the temperature difference between the ambient temperature and the cooler box room temperature rises. Consequently, applying Eq. (3) results in the increase in conduction heat transfer rate, as shown in Fig. 10. Furthermore, without water volume, the cooler box room temperature that can be achieved is lower than that with water volume. As a result, the conduction heat transfer rate is higher when without water volume. Nevertheless, the conduction heat transfer rate decreases with the increase in water volume. This is owing to the increased air temperature inside the cooler box room. When the air temperature in the cooler box room is high, then the temperature difference between inner and ambient temperatures decreases, consequently, the conduction heat transfer rate decreases.

Figure 11 shows the total heat transfer rate or the experimental cooling capacity at several water volumes. Similar to Q and Q_{wa} , Q_c decreases with the time but increases with the increased water volume. However, for the water volume of 0 ml and 600 ml, Q_c increases, and than after it reaches the peak value, it gets constant.

As mentioned in the data reduction, one parameter that can be used to evaluate the performance of the thermoelectric cooler box is *COP*, hence it is important to present the experimental *COP* as shown in Fig. 12. The *COP* increases with the time from 0 to of approximately 5000 s, and after that, it decreases with the time. Furthermore, the *COP* increases with an increase in water volume, however, its increment is not linear with the water volume. It can be seen in Fig. 12, that at 0 ml and 600 ml of water volumes the *COP* is almost the same at the time greater than 10000 s, while and at 1500 ml, 3000 ml, and 4500 ml the *COP* is not the same. Nevertheless, the increased *COP* with the water

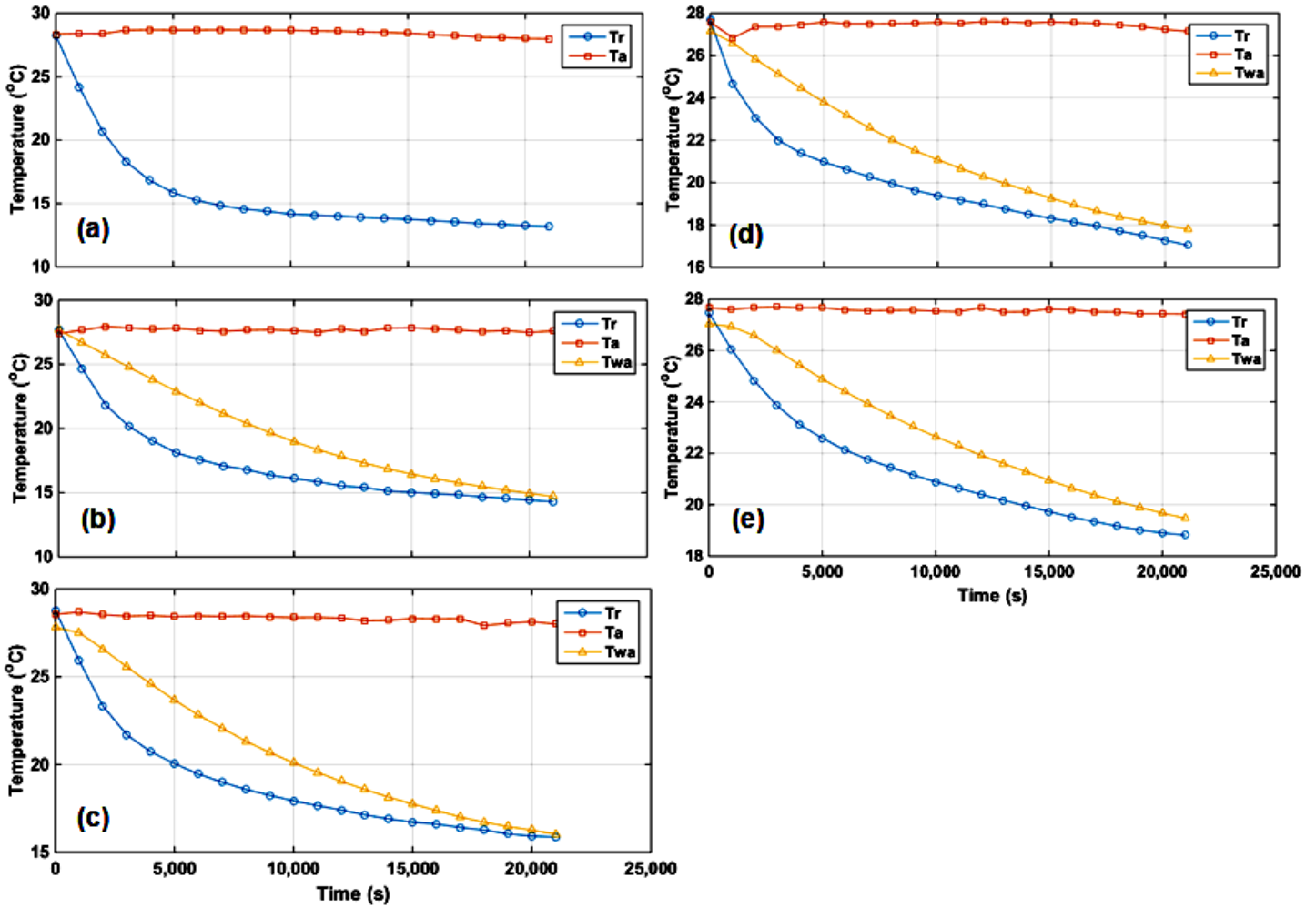


Fig. 4 Temperature trends versus observation time at several water cooling loads: (a) without water volume or 0 ml, (b) 600 ml, (c) 1500 ml and (d) 3000 ml and (e) 4500 ml at the same input power of 51.27 W. T_r is the air temperature ($^{\circ}\text{C}$), T_a is the ambient temperature ($^{\circ}\text{C}$), and T_{wa} is the drinking water temperature ($^{\circ}\text{C}$).

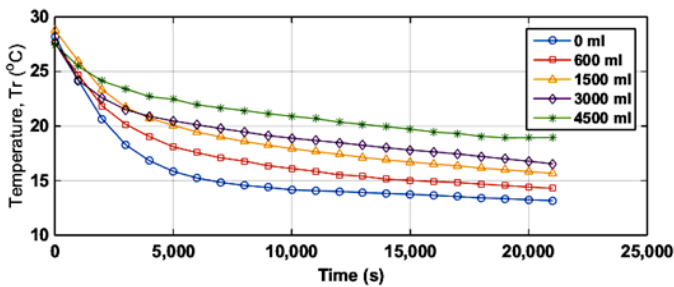


Fig. 5 Effect of cooling loads (drinking water) on the average room temperature

volume is due to the increased water mass. Higher the water mass, higher the cooling capacity, consequently higher the COP is found. Meanwhile, the decreased COP with the time is because of the decreased water and air heat transfer rates. The water and air heat transfer rates continue decreasing until they get a thermal equilibrium in the cooler box room. At the thermal equilibrium, the water and air heat transfer rates are close to zero and are replaced by the conduction heat transfer rate. The trend of the COP that decreases with the time was also found by Jugsujinda et al. (2011). Nevertheless, at the water volumes of 0 ml and 600 ml, the COP increases and then it gets

constant. This agrees with that found by Mirmanto et al. (2018a). This can happen when the cooling capacity is dominated by the conduction heat transfer rate. Moreover, in this study, the Carnot COP is also presented. It can be seen in Fig. 13. This type of COP just depends on the temperature, which is converted into Kelvin (K), and this can be expressed as:

$$COP_C = \frac{T_c}{T_h - T_c} \quad (17)$$

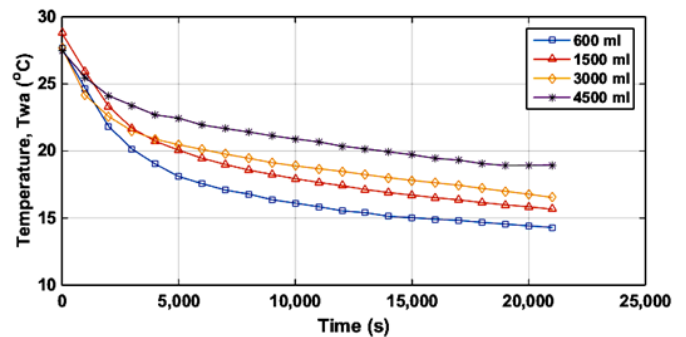


Fig. 6 Water temperatures versus observation time

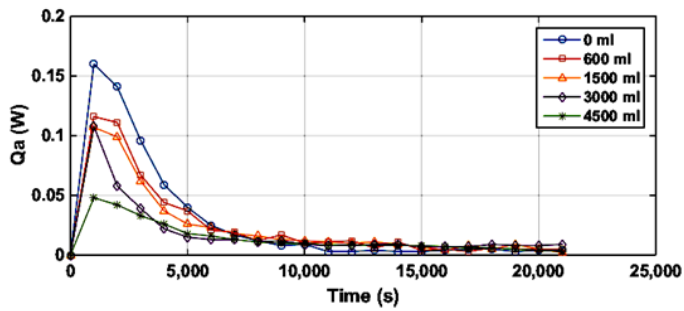


Fig. 7 Effect of water volume on the heat transfer rate of air at the power of 51.27 W

$$Q_c = Q_{c,max} (\Delta T_{max} - \Delta T) / \Delta T_{max} \quad (18)$$

COP_c is the Carnot coefficient of performance, $Q_{c,max}$ is the maximum cooling capacity (W), which is equal to 92 W, and ΔT_{max} is the maximum temperature difference, which is of approximately 66° for $T_h = 25^\circ C$, or $75^\circ C$ for $T_h = 50^\circ C$.

$$\Delta T_{th} = T_h - T_c \quad (19)$$

$$\Delta T_s = Ta - Tr \quad (20)$$

Figure 14 indicates that ΔT_{th} for the thermoelectric and ΔT_s for the system increases with the observation time, but decreases with the increase in water volume. The effect of water volume on ΔT of the system is very clear, while on ΔT_{th} is deteriorated at the water volumes of less than 1500 ml. This means that the experimental ΔT agrees with the theory, Eq. (18).

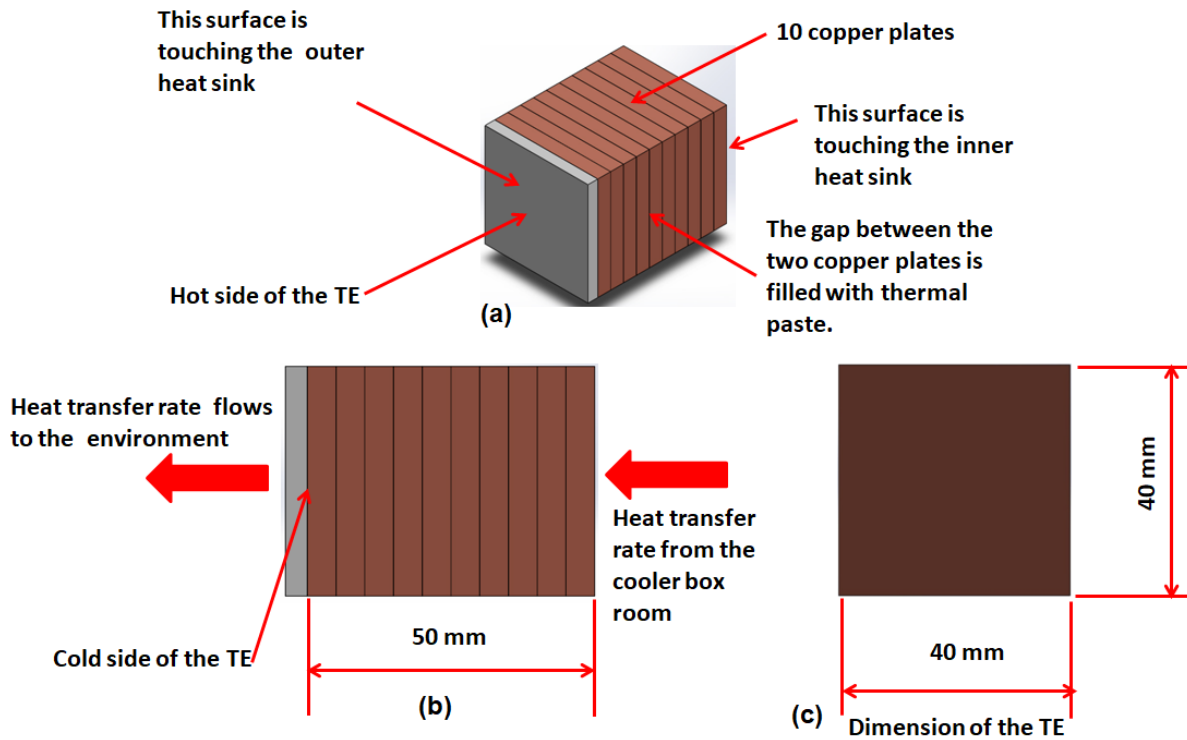


Fig. 8 Dimension of the copper block connector and the heat flow; (a) isometric view, (b) side view, (c) back view

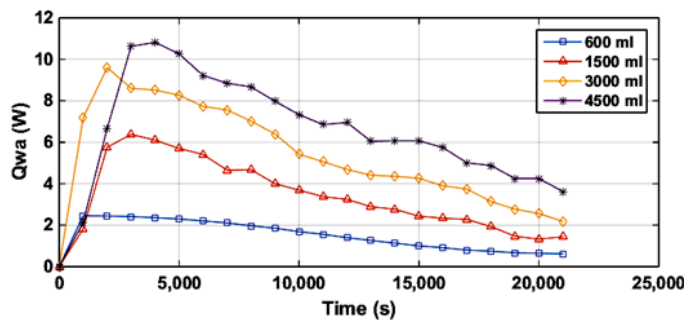


Fig. 9 Effect of cooling loads on water heat transfer rate at the power of 51.27 W

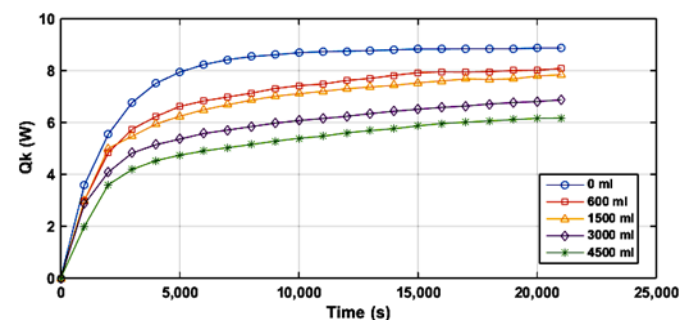


Fig. 10 Effect of cooling loads on conduction heat transfer rate

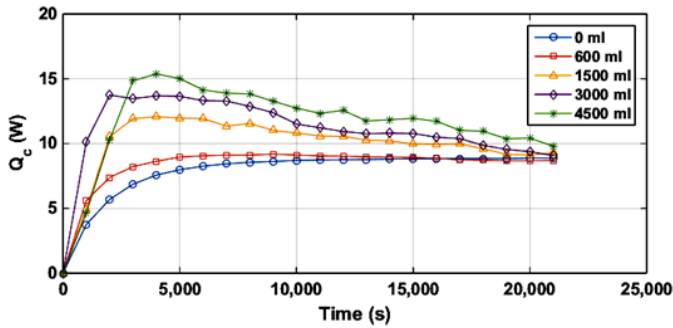


Fig. 11 Total experimental cooling capacity, Q_c

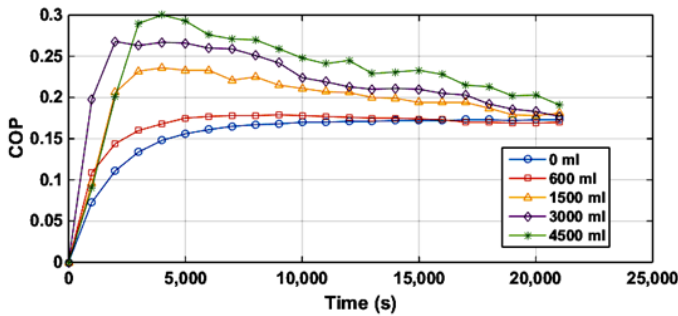


Fig. 12 Effect of cooling loads on the experimental COP.

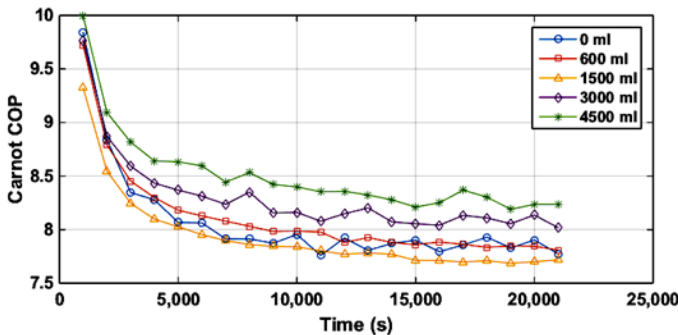


Fig. 13 Carnot COP

4. CONCLUSION

Experiments to investigate the effect of water volume on conduction heat transfer rate, cooling capacity and COP were performed using 3 identical thermoelectrics with power of 51.27 W and cooler box as the cooler box room. Some findings that have not been yet explained in the available published papers are: the deteriorated water volume effect on the heat transfer rate flowing from the air; the increased heat capacity due to the increase in water volume; and the trends of the conduction heat transfer rate flowing into the cooler box room.

In the future, the copper connectors should be replaced with a copper/ aluminum beam so that the more heat can be transferred.

ACKNOWLEDGMENTS

The authors would like to acknowledge the Mechanical Engineering Department, Mataram University for the facility and people who have helped in conducting the experiments and writing the manuscript.

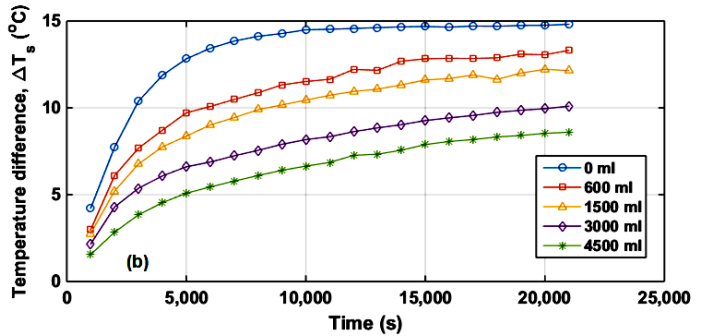
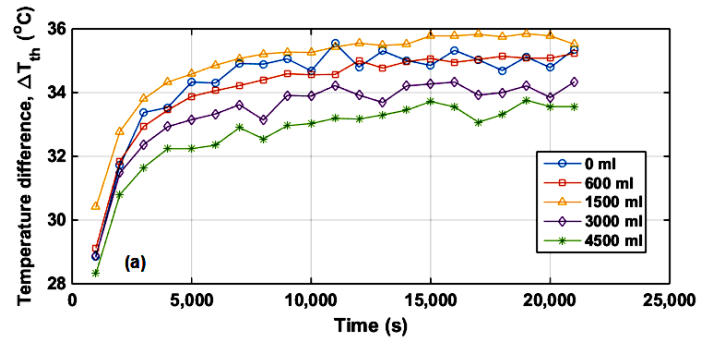


Fig. 14 Temperature difference, ΔT : (a) thermoelectric, (b) system

NOMENCLATURE

| | |
|------------------|--|
| A | ampere meter, a device to measure the current |
| A | heat transfer area (m ²) |
| c_p | specific heat (J/kg°C) |
| dT | temperature difference (°C) |
| dx | the wall thickness (m) |
| I | current (A) |
| i | segment |
| k | thermal conductivity (W/m°C) |
| m | air or water mass (kg) |
| P | power (W) |
| Q | heat transfer rate (W) |
| Q_c | cooling capacity (W) |
| Q_{cmax} | maximum cooling capacity (W) |
| R_{c+g} | thermal resistance of the connector (°C/W) |
| R_{hf} | force convection heat transfer coefficient (°C/W) |
| R_{ih} | thermal resistance of the inner heat sink (°C/W) |
| R_{oh} | thermal resistance of the outer heat sink (°C/W) |
| T | temperature (°C) |
| T_a | ambient temperature (°C) |
| T_f | film temperature (°C) |
| T_{hc} | temperature at the gap between the inner heat sink and copper block (°C) |
| T_{ih} | inner heat sink temperature (°C) |
| T_{oh} | outer heat sink temperature (°C) |
| T_r | average air temperature inside the cooler box room (°C) |
| T_{sf} | styrofoam layer surface temperature (°C) |
| T_{sp} | plastic layer surface temperature (°C) |
| T_{ss} | temperature of the stainless steel layer surface (°C) |
| T_{wa} | water temperature (°C) |
| ΔT | temperature difference (°C) |
| ΔT_{max} | maximum temperature difference (°C) |
| t | time (s) |
| V | voltmeter, a device to measure the voltage |
| V | voltmeter, voltage (V) |

Subscript:

c cold

| | |
|-----------|-------------------|
| <i>h</i> | hot |
| <i>i</i> | the time <i>i</i> |
| <i>in</i> | input |
| <i>k</i> | conduction |
| <i>s</i> | system |
| <i>wi</i> | inner wall |
| <i>wo</i> | outer wall |

Abbreviation

| | |
|-----|---------------------------------|
| ADC | ampere direct current |
| COP | coefficient of performance |
| DAQ | data acquisition (data logger) |
| DC | direct current |
| NI | National Instrument |
| RTD | resistance temperature detector |
| TE | thermoelectric |
| VDC | volt direct current |

REFERENCES

- Abdul-Wahab, S.A.A., Elkamel, A., Al-Damkhi, A.M., Al-Habsi, I.A., Al-Rubai'ey, H.S., Al-Battashi, A.K., Al-Tamimi, A.R., Al-mamari, K.H., and Chutani, M.U., 2009, "Design and Experimental Investigation of the Portable Solar Thermoelectric Refrigerator", *Renewable Energy*, **34**, 30-34.
<https://doi.org/10.1016/j.renene.2008.04.026>
- Ananta, H., Padang, Y.L., and Mirmanto, 2017, "Unjuk Kerja Kulkas Termoelektrik dengan Rangkaian Seri dan Paralel pada Beban Air 1500 ml", *Dinamika Teknik Mesin*, **7(2)**, 80-86.
<https://doi.org/10.29303/dtm.v7i2.157>
- Atik, K., and Yildiz, Y., 2012, "An Experimental Investigation Of A Domestic Type Solar TE cooler", *Energy Sources, Part A: Recovery, Utilization, and Environmental Effects*, 645-653.
<https://doi.org/10.1080/15567031003627989>
- Attey, G.S., 1998, "Enhanced Thermoelectric Refrigeration System COP through Low Thermal Impedance Liquid Heat Transfer System", *17th International Conference Thermoelectrics IEEE*, 519-524.
<https://doi.org/10.1109/ICT.1998.740431>
- Cengel, Y.A., and Boles, M.A., 2006, "Thermodynamics: An Engineering Approach", *5th edition, McGraw-Hill*, New York, USA.
- Ghoshal, U., Ghoshal, S., McDowell, C., and Shi, L., 2002, "Enhanced TE Cooling at Cold Junction Interfaces", *Applied Physics Letter*, **80(16)**, 3006-3008.
<https://doi.org/10.1063/1.1473233>
- Holman, J.P., 1997, "Heat Transfer", 8th Edition, McGraw-Hill Inc., USA.
- Jugsujinda, S., Vora-ud, A., and Seeawan, T., 2011, "Analyzing of Thermoelectric Refrigerator Performance", *Procedia Engineering*, **8**, 154-159.
<https://doi.org/10.1016/j.proeng.2011.03.028>
- Lee, H.J., Anoop, G., Kim, C., Park, J.W., Choi, J., Kim, H., Kim, Y.J., Lee, E.J., Lee, S.G., Kim, Y.M., Lee, J.H., and Jo, J.Y., 2015, "Enhanced TE Performance of PEDOT: PSS/PANI-CSA Polymer Multilayer Structures", *Energy & Environmental Science*, **0(1-3)**, 1-7.
<https://doi.org/10.1039/C5EE03063C>
- Lu, T., Zhou, J., Li, N., Yang, R., and Li, B., 2014, "Inhomogeneous Thermal Conductivity Enhances Thermoelectric Cooling", *AIP ADVANCES*, **4.124501**, 1-8.
<http://dx.doi.org/10.1063/1.4903547>
- Manohar, K., and Adeyanju, A.A., 2014, "Comparison of the Experimental Performance of A Thermoelectric Refrigerator with A Vapour Compression Refrigerator", *Int. J. Technical Research and Application*, **2(3)**, 01-05.
- Manohar, S.R., Mallikarjun, R.N., Sidharam, G.A., Vyankatesh, G.P., and Dulange, S.R., 2016, "Analysis of Solar Refrigeration System Using Thermo Electric Cooling (TEC) Module", *Navateur Publications Journal Of Innovation In Engineering, Research And Technology*, 1-9.
- Mirmanto, Sutanto, R., and Putra, D.K., 2018a, "Unjuk Kerja Kotak Pendingin Termoelektrik dengan Varuasi Laju Aliran Massa Air Pendingin", *Jurnal Teknik Mesin*, **7(1)**, 44-49.
<http://dx.doi.org/10.22441/jtm.v7i1.2307>
- Mirmanto, Alit, I.B., Sayoga, I.M.A., Sutanto, R., Nurchayati, Mulyanto, A., 2018b, "Experimental Cooler Box Performance Using Two Different Heat Removal Units: A Heat Sink Fin-Fan, and A Double Fan Heat Pipe", *Frontier in Heat and Mass Transfer*, **10(34)**, 1-7.
<http://dx.doi.org/10.5098/hmt.10.34>
- Rawat, M.K., Chattopadhyay, H., and Neogi, S., 2013, "A Review on Developments of Thermoelectric Refrigeration and Air Conditioning Systems: A Novel Potential Green Refrigeration and Air Conditioning Technology", *Int. J. Engineering Technology and Advanced Engineering*, **3**, 362-367.
- Reddy, N.J.M., 2016, "A Low Power, Eco-Friendly Multipurpose Thermoelectric Refrigerator", *Front Energy*, **10(1)**, 79-87.
<https://doi.org/10.1007/s11708-015-0380-8>
- Villasevil, F.X., Lopez, A.M., and Fisac, M., 2013, "Modeling and Simulation of A Thermoelectric Structure with Pellets of Non-Standard Geometry And Materials", *Int. J. Refrigeration*, **36(5)**, 1570-1575.
<https://doi.org/10.1016/j.ijrefrig.2013.02.014>
- Yang, J.J., Tan, S.J., and Wu, B.X., 1991, "Development and Effect Test of KWX-1 Portable Medical Refrigerator", *Medical Equipment*, **3**, 14-15.
- Yu, J., and Wang, B., 2009, "Enhancing the Maximum Coefficient of Performance of Thermoelectric Cooling Modules Using Internally Cascaded Thermoelectric Couples", *Int. J. Refrigeration*, **32**, 32-39.
<https://doi.org/10.1016/j.ijrefrig.2008.08.006>